Electromechanical Model of Flexible Arm Flexible Root Manipulator Rotated by a DC Motor

Ahmed Abed
Public Authority of Applied Education and Training/ Collage of Technological Studies
Automotive and Marine Department

Abstract

This paper presents a mathematical dynamic model of a flexible arm-flexible-root manipulator driven by a DC motor. The mechanical system equations of motion are derived using the Lagrangian dynamics, the assumed modes method and the condition of inextensibility. The simple DC motor theory is adopted and augemented to the mechanical model through the motor torque and hub angular velocity. The system produced is a nonlinear model that is electromechanically coupled and presented in state space. This model enables studying the flexible arm dynamics through monitoring the motor electrical variables. Simulation results on the effects of root flexibility and the arm attachment angle on the system electromechanical dynamics are presented and discussed. The motor armature current spectrums captured the arm vibration frequency.

1. Introduction

Rotating flexible arms have attracted the attention of many researchers in the area of dynamics and control due to the increasing need to operate light weight structures with precise positioning and control. Rotating flexible members are usually operated using various types of electrical motors that have inherited dynamic characteristics. A model that represents the coupled electrical motor and the rotating flexible arm dynamics is desirable in the design and operation of such systems. This model is expected to provide a two ways dynamic interaction that enables the simulation of the coupled electromechanical system. More over the model aims at monitoring the flexible arm vibration through reflections to the electrical current.

The effect of rotation on the natural frequencies and mode shapes of a rotating beam was reported earlier by Shilhansi [1] and Prudli [2]. These studies have shown that the rotation speed strengthens the beam and produces high natural frequencies. Likins [3] reported a study on the mathematical modeling of spinning elastic bodies. In the same direction, Kaza and Kavternik [4] reported results of a study on the non-linear flap-lag-axial equations of a rotating beam. They addressed the problem of axial rigidity and the shortening due to transverse deflection. Kaza and Kavternik [4] summarized the four methods for accounting for the beam axial rigidity. Stephen and Wang [5] studied the effect of uniform high-speed rotation on the stretching and bending of a rotating beam. They accounted for the beam rotation dynamics in terms of a tensile force that produced axial stress on the beam. In the aforementioned studies, the effect of rotation was taken as kinematics variable in the form of angular velocity and angular acceleration to be given to the elastic equations, which in turn are solved for the natural frequencies and mode shapes. Kane et al. [6] studied the dynamic behavior of a cantilever beam that is attached to rigid base and performing specified motion of rotation and translation. In their work the elastic degrees of freedom included beam axial extension, bending in two planes, torsion, shear displacement and wrapping. The model is a general three-dimensional elastic beam model; however, the two-way coupling between the rigid body motion and elastic deflections was not accounted for because only specified rigid body motions were considered.

The multi-body dynamic approach, in which the rigid motion and flexible deformations are modeled in their coupled format, has attracted many researchers. Baruh and Tadikonda [7] reported some issues in the dynamics and control of flexible robot manipulators. They addressed the problem of axial shortening due to bending deformations by considering the shortening in their kinetic energy expression. Their results have shown that the flexibility of the rotating arm has changed the desired final rigid body position. Tadikonda and Chang [8] reported the effect of end load, due to chain connections on the geometric stiffening. Yigit et al. [9] studied the dynamics of a radially rotating beam with impact. They modeled the

rigid body motion and the beam elastic co-ordinates using a partial differential equation and Galerkin's method of approximation. The effect of beam axial shortening due to bending deformation and the resulting beam stiffening was considered in their equations. The model showed linear inertial coupling between the beam rigid body rotation and the its elastic deflections and the effect of shortening appeared as function of square of beam rigid body rotating speed in the stiffness term. Pan et al. [10] reported a dynamic model and simulation results of a flexible robot arm with prismatic joint. They accounted for the effect of axial shortening using a virtual work term added to the elastic potential energy. El-Absy and Shabana [11] studied the geometric stiffens for a rotating beam using different approaches. They introduced the effect of longitudinal deformation due to bending, in the equations of motion, using the principle of virtual work. Al-Bedoor [12] studied the effects of shaft torsional flexibility on the dynamics of rotating blades. The effect of axial shortening was accounted for using the virtual work in the form of added potential energy due to the centrifugal forces. Numerical simulations have shown that the flexibility and the stiffening effect contribute to the rigid body inertia by quadratic terms. The effect of inextensibility condition on the dynamics of rotating flexible arm and its associated dynamic non-linearity was recently reported by Al-Bedoor and Hamdan [13]. Their numerical results showed that the non-linear terms could improve the stability of the system dynamic behaviour.

Up to authors knowledge the electromechanical modeling of a flexible arm driven by an electrical motor is not available in the open literature. Moreover, most of the published models on rotating flexible arms adopted the cantilever end condition and the beam model that is radially attached to the hub.

In this paper, the dynamics of a rotating flexible arm that is driven by DC motor is developed. The arm is modeled using Euler-Bernoulli beam theory and the attachment root general condition is modeled using a torsional spring with a limiting case of cantilever beam end condition. The Lagrangian

dynamics in conjunction with the assumed model method is used in developing the equations of motion. The effect of shortening in accounted for by imposing the inextensibility condition. The DC motor model is coupled with the arm rigid body and flexible degrees of freedom model. The effect of payload is considered by consistently deriving its associated dynamic model. The voltage input to the motor is used to rotate the arm to a pre-designed angular position with imposed conditions on the motion parameters. The arm angular position, angular velocity and vibration are monitored simultaneously with the motor armature current. The model and the simulation results are presented and discussed.

2. Model Development

2.1 Description and Model Assumptions

A schematic diagram of a rotating flexible arm driven by an electrical motor is shown in Figure 1. The hub is assumed to be rigid and the flexible arm is attached to the hub with an attachment angle η as shown in Figure 2. The arm is assumed to be inextensible, i.e., there is no axial deformation. The coordinate systems used in developing the model are shown in Figure 2. Where in, XY is the inertial reference frame and xy is a rotating coordinate system attached to the hub such that its x-axis is directed along the undeformed configuration of the arm. The assumptions used in developing the model can be listed as follows:

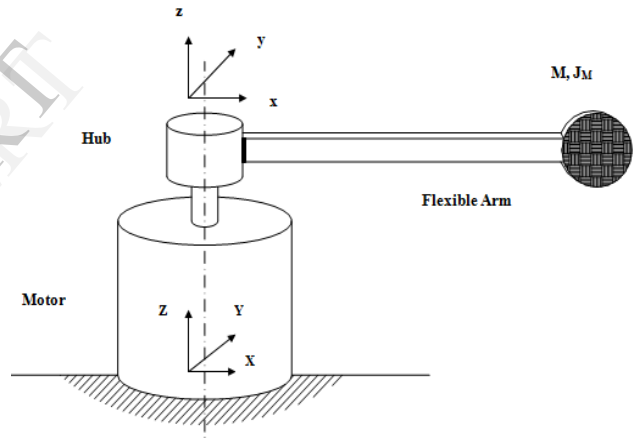

Figure 1. Schematic diagram of a rotating arm system.

- The hub is assumed to be rigid with radius R_H and rotating about the Z-axis.
- The arm is operated in the horizontal plane so the effect of gravity is neglected.
- The cross section of the arm is assumed to be small compared to its length. The beam is slender and the Euler-Bernoulli beam theory is adopted. The effect of shear deformation and rotary inertia are neglected.
- The effect of axial shortening due to arm transverse deformation is accounted by the inextensibility condition.

2.2 Kinetic Energy

To develp the kinetic energy expression for the rotating arm-hub system, the deformed configuration of the arm, shown in Figure 2, is used. The global position vector of a material point P, located on the arm can be written as:

$$R_P = R_H + [A(\eta)][A(\theta)]r_P \qquad (1)$$

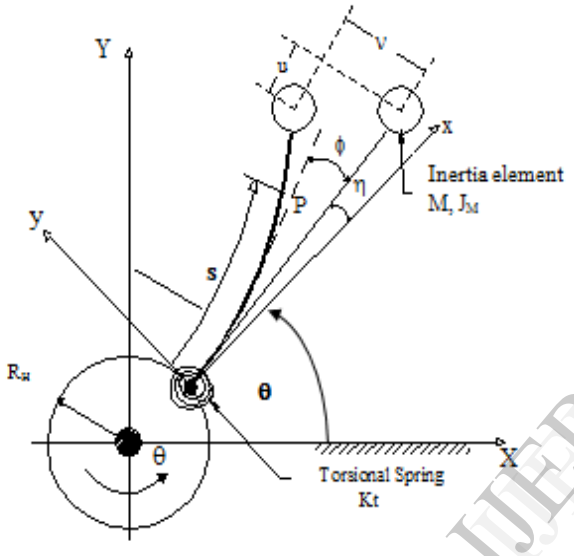

Figure 2. Deformed configurations of the arm-hub system and coordinate system.

where r_p is the position vector of a material point *P* in the hub coordinate system xy, *[A(θ)]* is the rotational transformation matrix from the hub coordinates system *xy* to the inertial reference frame XY, *[A(η)]* is the rotational transformation matrix that takes care of the constant attachment angle η and R_H is the position vector of the origin of the hub coordinates system xy in the inertial frame reference XY.

The position vector of the arbitrary material point *P* in the xy coordinate system can be written in the form:

$$r_P = (s-u)i + vj \qquad (2)$$

Where $u(s,t)$ is the axial shortening due to bending deformation and $v(s,t)$ is the transverse deflection of the material point P measured with respect to the hub coordinates system. The position of the origin of the *xy* coordinate system in the XY inertial frame can be written as:

$$R_H = R_H \cos\theta\, I + R_H \sin\theta\, J \qquad (3)$$

The rotational transformation matrices, for planer motion corresponding to the rotation θ and the attachment angle η, can be expressed respectively, as:

$$A(\theta) = \begin{bmatrix} \cos\theta & -\sin\theta \\ \sin\theta & \cos\theta \end{bmatrix} \quad and \quad A(\eta) = \begin{bmatrix} \cos\eta & -\sin\eta \\ \sin\eta & \cos\eta \end{bmatrix} (4)$$

Where θ is the rigid hub rotation and η is the attachment angle.

To develop mathematical expression for the system kinetic energy, the velocity vector of the arbitrary material point on the arm span can be obtained by differentiating equation (1) with respect to time as

$$\dot{R}_P = \dot{R}_H + [A(\eta)]\,[A(\theta)]\;\dot{r}_P + \dot{\theta}\,[A(\eta)]\,[A_\theta(\theta)]r_P \qquad (5)$$

follows:
where $A_\theta(\theta) = [\delta A/\delta\theta]$. Substituting equations (2), (3) and (4) and their derivatives into equation (5), the vleocity vector of the material point in the inertial

$$\dot{R}_P = \begin{Bmatrix} -\alpha\sin\theta + \beta\cos\theta \\ \alpha\cos\theta + \beta\sin\theta \end{Bmatrix} \qquad (6)$$

reference frame can be expressed as:

The kinetic energy for the arm that has constant

$$\alpha = \dot{\theta}(R_H + (s-u)(\cos\eta - v\sin\eta) + \dot{v}\cos\eta - \dot{u}\sin\eta$$
$$\beta = -\dot{\theta}((s-u)\sin\eta + v\cos\eta) - \dot{v}\sin\eta - \dot{u}\cos\eta \qquad (7)$$

$$U_A = \frac{1}{2} m_A \int_0^1 \dot{R}_P{}^T . \dot{R}_P d\zeta \qquad (8)$$

properties and uniform cross section can be represented in the form [13]:

where $m_A = \rho l$ is the arm mass assuming uniform cross section, $\dot{R}_P$ is the velocity vector of a material point P and, ζ = s/*l* is the dimensionless axial position of point P.

The kinetic energy of the hub which is assumed to be a rigid uniform disk with radius R_H, mass m_H and rotating with angular velocity $\dot{\theta}$ can be written as [13]:

$$U_H = \frac{1}{4} m_H R_H{}^2 \dot{\theta}^2 \qquad (9)$$

The kinetic energy of the payload represented by mass M and rotary inertia J_M attached at the free end of the arm can be expressed as:

$$U_M = \frac{1}{2} M(\dot{R}_M{}^T . \dot{R}_M) + \frac{1}{2} J_M(\dot{\theta} + \dot{\phi})^2 \qquad (10)$$

Where M is the attachment mass $\dot{R}_M$ is the velocity vector of payload, J_M is the attached rotary inertia and ϕ the slope of the deformed arm, at its tip. The total kinetic energy of the system is composed of the kinetic energy of the hub, the arm and the payload as follows:

$$U = U_H + U_A + U_H \qquad (11)$$

Substituting equations (8),(9) and (10) into equation (11) kinetic energy of the Arm-hub-mass system can be written as:

$$U = \frac{1}{2} m_A \int_0^1 [\dot{\theta}^2(((s-u)+R_H)^2 + v^2) + 2\dot{\theta}(\dot{v}(s-u) + \dot{v}R_H + \dot{u}v) + \dot{v}^2 + \dot{u}^2] d\zeta +$$
$$\frac{1}{2} M[\dot{\theta}^2(((s-u)+R_H)^2 + v^2) + 2\dot{\theta}(\dot{v}(s-u) + \dot{v}R_H + \dot{u}v) + \dot{v}^2 + \dot{u}^2]_{\zeta=1} +$$
$$\frac{1}{4} m_H R_H{}^2 \dot{\theta}^2 + \frac{1}{2} J_M(\dot{\theta} + \dot{\phi})^2 \Big|_{\zeta=1} \qquad (12)$$

2.3 The Potential Energy Expressions

The system potential energy is constituted of the arm elastic strain energy and potential energy stored in the torsional spring at the arm root. The arm is assumed to be rotating in the horizontal planes that result in no gravitational potential energy.

$$V = \frac{EIl}{2} \int_0^1 R^2 d\zeta + \frac{1}{2} K_t (v')^2 \Big|_{\zeta=0} \qquad (13)$$

where R is the radius of curvature of the arm neutral axis, and K_t is the root stifness of the arm.

2.4 The Inextensibility Condition

To take care of the effect of shortening due to beam transverse deflection the inextensibility condition is adopted [13]. For the two dimensional arm shown in Figure3, the inextensibility condition dictates that the axial shortening $u(s,t)$ can be represented as:

$$\lambda u(\zeta, t) = \zeta - \int_0^1 \cos[\phi(\eta, t)] d\eta \qquad (14)$$

Where $\zeta = s/l$ and $\lambda = 1/l$, $\sin\phi = dv/ds$ and $\cos\phi = \sqrt{1-\sin^2\phi}$. Expanding the term $\sqrt{1-(\lambda v'^2)}$ in a power series, assuming that $(\lambda v`^2) << 1$, the axial position of material point can be represented as:

$$u = \frac{1}{2} \int_0^1 [\lambda v'^2 + \frac{1}{4} \lambda^3 v'^4] d\zeta \qquad (15)$$

where prime is the derivative with respect to the dimentionless parameter ζ.

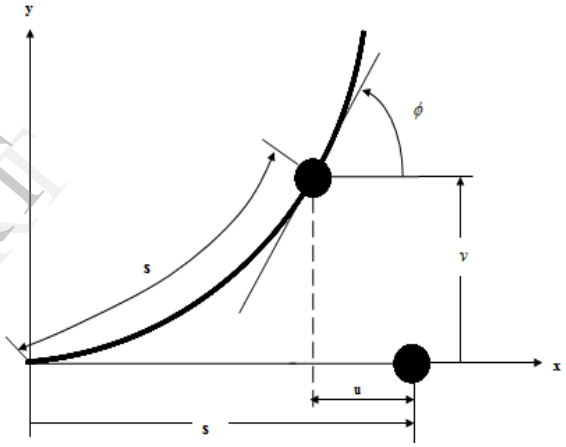

Figure 3. Deflected configuration of the arm segment.

Differentiating equation (15) withrespect to time yields:

$$\dot{u} = \frac{1}{2} \frac{d}{dt} [\int_0^1 [\lambda v`^2 + \frac{1}{4} \lambda^3 v`^4] d\eta] \qquad (16)$$

The non-linear curvature can be written in the following form:

$$R = \phi' \qquad (17)$$

$$\sin\phi = \lambda v' \qquad (18)$$

$$R^2 = \lambda^4 v''^2 + \lambda^6 v^2 v''^2 \qquad (19)$$

The potential energy can be written in the form:

$$V = \frac{EIl}{2} \int_0^1 (\lambda^4 v''^2 + \lambda^6 v'^2) d\zeta + \frac{1}{2} K_t v'^2 \qquad (20)$$

2.5 The Assumed Modes Method

Using kinetic and potential energies equations (12) and (20) respectively, the Lagrangian of the system L can be obtained as:

$$L = U - V = \frac{1}{2} m_A \int_0^1 [\dot{\theta}^2(((s-u)+R_H)^2 + v^2) + 2\dot{\theta}(\dot{v}(s-u) + \dot{v}R_H + \dot{u}v) + \dot{v}^2 + \dot{u}^2]d\zeta +$$
$$\frac{1}{2} M[\dot{\theta}^2(((s-u)+R_H)^2 + v^2) + 2\dot{\theta}(\dot{v}(s-u) + \dot{v}R_H + \dot{u}v) + \dot{v}^2 + \dot{u}^2]_{\zeta=1} +$$
$$\frac{1}{4} m_H {R_H}^2 \dot{\theta}^2 + \frac{1}{2} J_M (\dot{\theta} + \dot{\phi})^2\Big|_{\zeta=1} - \frac{EIl}{2}\int_0^1 (\lambda^4 v''^2 + \lambda^6 v'^2)d\zeta + \frac{1}{2} K_t v'^2 \quad (21)$$

The system of equation (21) contains the beam continuous deflection represented by $v(\zeta,t)$. In order to separate the spatial and temporal dependence of the beam deflection, the assumed modes method is utilized in which the beam deflection $v(\zeta,t)$ can be presented in the form:

$$v(\zeta,t) = \sum \phi_i(\zeta) q_i(t) \qquad (22)$$

where $\phi_i(\zeta)$ is the normalized, assumed deflection shape of the arm-mass that is found using eigenvalue analysis, and $q(t)$ is an unknown time dependent generalized deflection.

The arm-hub mass mode shape $\phi_i(\zeta)$ is found based on the assumption of non-rotating linear beam which can be written in the form [14]:

$$\phi_i(\zeta) = A\sin(P_i\zeta) + B\cos(P_i\zeta) + C\sinh(P_i\zeta) + D\cosh(P_i\zeta) \qquad (23)$$

where A,B,C and D are arbitrary constants to be determined from the following four boundary conditions:

$$\phi(0) = 0$$
$$EI\phi''(0) = K_t\phi'(0)$$
$$\phi''(1) = a_3 {p_i}^4 \phi'(1)$$
$$\phi'''(1) = -a_2 {p_i}^4 \phi(1)$$

where $a_2 = M/m_B$, $a_3 = J_M/[m_B\, l^2]$ and P_i is the i-th dimensionless frequency parameter of the non-rotating linear arm-mass.

2.6 Equations of Motion

Upon substituting equation (22) the expression for the system Lagrangian will take the form:

$$L = \frac{m_A l^2}{2}\{\beta_1\dot{\theta}^2 + \beta_2\dot{q}^2 - \beta^2\beta_3 q^2 + \beta_5\dot{\theta}^2 q^4$$
$$+ \beta_6\dot{\theta}\dot{q} + \beta_7\dot{\theta}\dot{q}q^2 + \beta_8 q^2\dot{q}^2 - \beta^2\beta_9 q^4$$
$$+ \beta_{10}\dot{\theta}\dot{q}q^4 + \beta_{11}\dot{\theta}\dot{q}q + \beta_{12}\dot{\theta}\dot{q}q^3 + \beta_{13} q\dot{\theta}^2\} \qquad (24)$$

where the different coefficients have integral definitions in the terms of system parameters and beam assumed deflection mode shape as given in Appendix A.

The Lagrangian of the Arm-hub-mass system given in equation (24) is expressed in terms of the $\dot{\theta}$, q, $\dot{q}$ and β_i, i=1,.....,13. The values of β_i are independent from time and they are based on mode shape given in equation (23).

Using the virtual work method, the external torque T applied at the hub can be represented in the form:

$$\delta W = T\,\delta\theta \qquad (25)$$

By applying the Euler-Lagrange equation to the system Lagrangian equation (24) for $\dot{\theta}$, q, $\dot{q}$ and θ system equations of the motion are obtained as:

$$\begin{bmatrix}\alpha_{11} & \alpha_{12}\\ \alpha_{21} & \alpha_{22}\end{bmatrix}\begin{bmatrix}\ddot{\theta}\\ \ddot{q}\end{bmatrix} + \begin{bmatrix}0 & 0\\ 0 & \alpha_{23}\end{bmatrix}\begin{bmatrix}\theta\\ q\end{bmatrix} + \begin{bmatrix}\alpha_{13}\dot{q}\dot{\theta} + \alpha_{14}\dot{q}^2\\ \alpha_{24}\dot{\theta}^2\end{bmatrix} = \begin{bmatrix}\frac{2T}{m_A l^2}\\ 0\end{bmatrix} \quad (26)$$

$$\alpha_{11} = 2(\beta_1 + \beta_{13}q + \beta_4 q^2 + \beta_5 q^4).$$
$$\alpha_{12} = \beta_6 + \beta_{11}q + \beta_7 q^2 + \beta_{12}q^3.$$
$$\alpha_{13} = 2(\beta_{13} + 2\beta_4 q + 4\beta_5 q^3).$$
$$\alpha_{14} = \beta_{11} + 2\beta_7 q + 3\beta_{12}q^2 + 4\beta_{10}q^3.$$
$$\alpha_{21} = \beta_6 + \beta_{11}q + \beta_{10}q^4 + \beta_7 q^2 + \beta_{12}q^3.$$
$$\alpha_{22} = 2(\beta_2 + \beta_8 q^2).$$
$$\alpha_{23} = 2(\beta^2\beta_3 + 2\beta^2\beta_9 q^2 + \beta_8\dot{q}^2).$$
$$\alpha_{24} = -(\beta_{13} + 2\beta_4 q + 4\beta_5 q^3).$$

Equation (27) model the dynamics of a flexible rotating arm carrying a pay load at its tip. The first coefficient matrix is the inertia matrix which is dynamically coupled. The entries of the inertia matrix contain the dependent variable q and are nonlinear. The second coefficient matrix is the stiffness matrix that contain

nonlinear terms of the dependent variable *q* and its time derivative.The third term is the nonlibnear vector that contains the nonlinear effect known as the coriolis effect as well as the effect of beam rotation on the beam stiffness known as stiffening effect.

3. The Electromechanical Model

Schematic diagram of a rotating flexible arm driven by an electrical motor is shown in Figure 4. The selected motor for this model is a DC motor with its standard equivalent circuit shown in Figure 5.

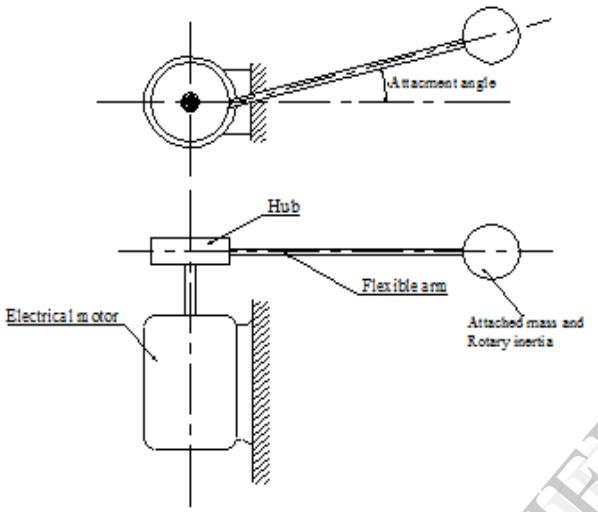

Figure 4. Schematic of electromechanical system.

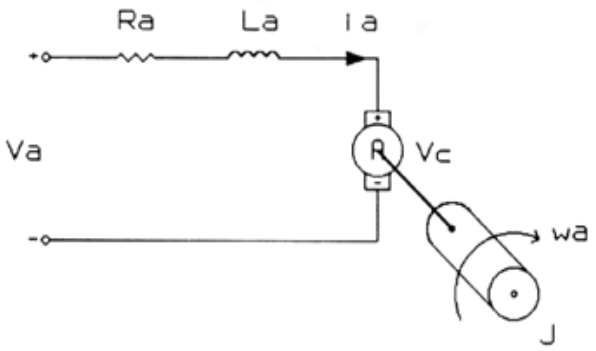

Figure 5. Electrical representation of a dc motor.

The electromagnetic torque is proportional to the current through the armature-winding constant and can be written as:

$$T = K_m i_a \qquad (27)$$

The time differential equation of the armature current can be written as:

$$\frac{d}{dt} i_a = -\frac{R_a}{L_a} i_a - \frac{K_v}{L_a} \omega_a + \frac{V_a}{L_a}$$

$$\frac{d}{dt} \omega_a = \frac{K_m}{J} i_a - \frac{B}{J} \omega_a - \frac{T_L}{J} \qquad (28)$$

$$\frac{d}{dt}\begin{bmatrix} i_a \\ \dot{\theta}_a \end{bmatrix} = \begin{bmatrix} -\frac{R_a}{L_a} & -\frac{K_v}{L_a} \\ \frac{K_m}{J} & -\frac{B}{J} \end{bmatrix}\begin{bmatrix} i_a \\ \dot{\theta}_a \end{bmatrix} + \begin{bmatrix} \frac{1}{L_a} & 0 \\ 0 & -\frac{1}{J} \end{bmatrix}\begin{bmatrix} V_a \\ T_L \end{bmatrix} \qquad (29)$$

The electromechanical model has five first order ordinary differential equations. The coupling between mechanical and electrical variables depends on the linear terms such as the torque coefficient K_m which couples the motor torque with the coil current i_a and the back electromotive force coefficient K_v, and the coil applied voltage V_a with the angular velocity $\dot{\theta}$.

4. Numerical Simulation

The set of non-linear first order ordinary differential equations are simulated using the predictor corrector time marching numerical solver ode15s of the MATLAB package. The input voltage of the motor is designed using the inverse dynamics procedure to rotate the hub-rigid arm equivalent system to a pre-set target angular position θ_T within specified time interval. The physical parameters of the simulated system are given in Table 1.

Table 1. Arm-hub data.

Property	Value
Arm length *l*	1.0 m
Arm mass per uint length, ρ	1.35 kg/m
Arm flexural rigidity, EI	75.0 N.m^2
Hub radius, R_H	0.05m
Hub mass, m_H	3.18 kg

The DC motor parameters are its armature resistance R_a =1.25Ω, armature inductance L_a = 2.6mH, torque constant K_m= 0.056 Nm/A, voltage constant K_b = 0.056 V.s/rad, and the damping factor K_d= 0.0067 Nm.s/rad. Applying typical equivalent voltage shown in Figure 6, the system response is simulated and the results of angular position, angular velocity, tip deflection and

motor armature current are presented in graphical form for different system characteristics.

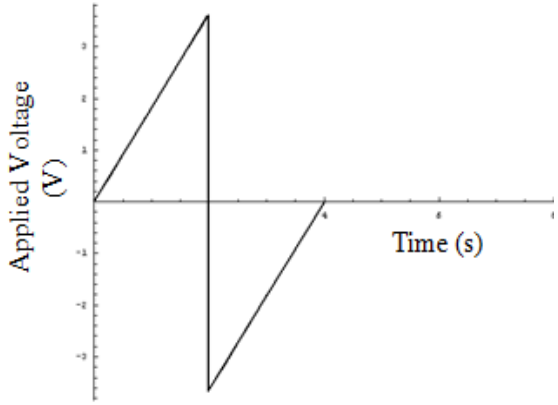

Figure 6. Voltage profile used to rotate the arm – mass-hub system π/4 rad in 4 sec.

The system response for the applied voltage to rotate the arm an angle of 45^o in 4 seconds is shown in Figure 7, as angular position, angular velocity, tip deflection and armature current variation with time. The system stiffness ratio $K_e = \frac{K_t l}{EI}$ is taken to be infinite that represents the cantilever condition and the attachment angle $\eta=0^o$. The response shows that the arm goes to its target position with residual fluctuations in the tip deflection and also in the armature current. Although the fluctuations in the armature current is small compared to the overall current ranges (-10A, 10A), it can be observed if zoomed after the current mean is returned to zero. The tip deflection and the armature current frequency spectrums are shown in Figure 8.

To investigate the effect of attachment angle η on the dynamics of the same arm, the model is run with all previous parameters except the attachment angle which is $\eta=45^o$ and the simulation results are compared in Figure 9. The associated tip deflection and armature current frequency spectrums are shown in Figure 10.

For small stiffness ratio K_e =0.2 (i.e. approaching hinge support), the system response is shown in Figure 11. The effect of reducing the root stiffness is reflected as fluctuation in the arm rigid angular position and velocity, increase in the tip deflection vibration amplitude. Moreover, the natural frequency of vibration is reduced to below 1 HZ as reflected by the frequency spectrums of Figure 12. The frequency spectrum of the armature current reflected exactly the tip arm vibration frequency with higher amplitude than the case with rigid root (cantilever) in the previous simulation. The effect of attachment angle is shown in Figure 11 and 12.

5. Conclusions

In this study a mathematical model for the coupled elecrtomechanical system is developed and simulated. The modeled system is constituted of a DC motor driving a flexible arm attached to a rigid hub through torsional spring to simulate root fixation problems. The arm flexibility is modeled using the Lagrangian dynamics in conjunction with the assumed modes method. The effect of arm shortening due to bending deformation is accounted for using the in-extensibility condition. The pay load effect is modeled as point mass and point inertia attached to the tip of the arm. The inverse dynamics procedure with the idealized motor model is used to find the needed voltage to rotate the arm to a prescribed target angular position. Simulation results showed that the effect of reducing the root flexibility increases the arm tip vibration amplitude and decrease its vibration frequency.

The result supports the idea that mechanical vibration is a load that can be reflected in the armature current. More experimental and theoretical studies on the electromechanical coupling, particularly using other types of motors are recommended.

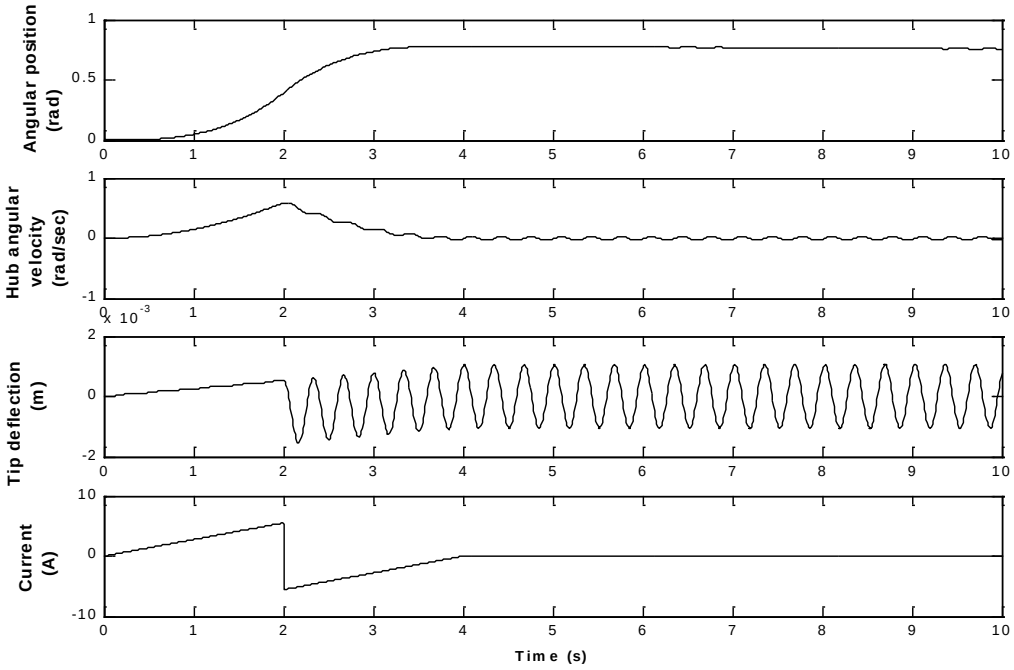

Figure 7. System response for Stiffness ratio $K_e = \infty$ and Attachment angle $\eta = 0$.

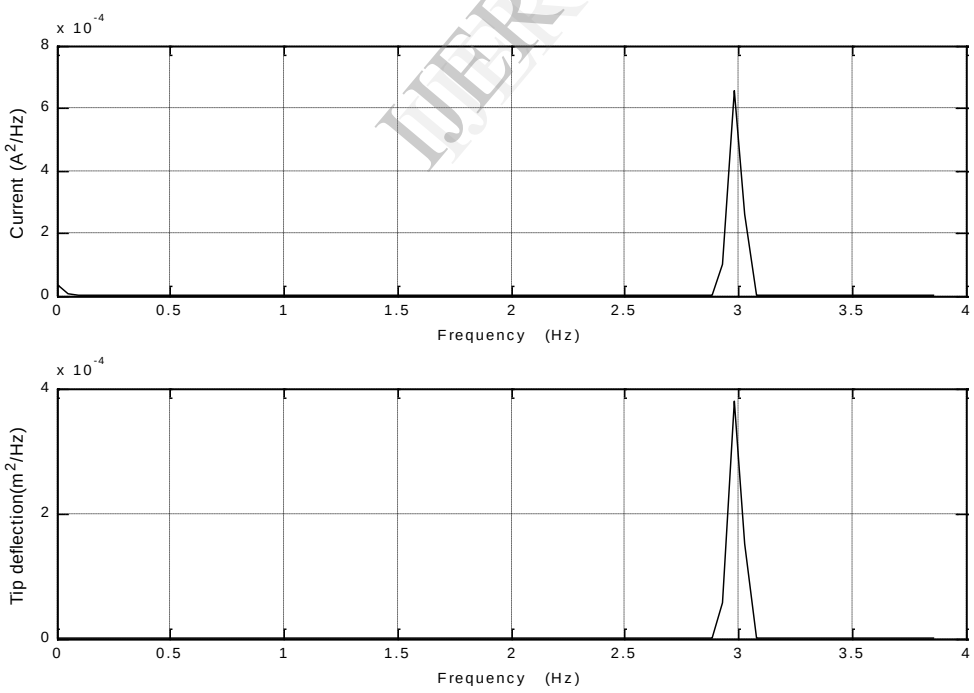

Figure 8. Frequency spectrums a) current signal and b) arm tip deflection.

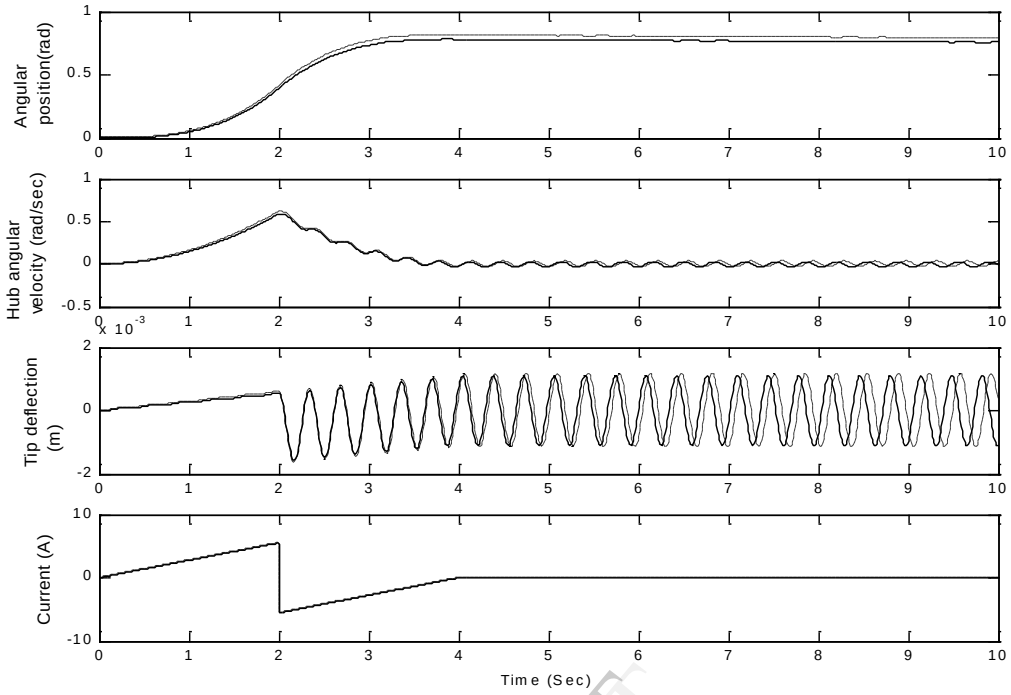

Figure 9. System response for stiffness ratio K_e = 100 and Attachment angle $\eta = 0^o$ (-) and $\eta = 45^o$ (-----).

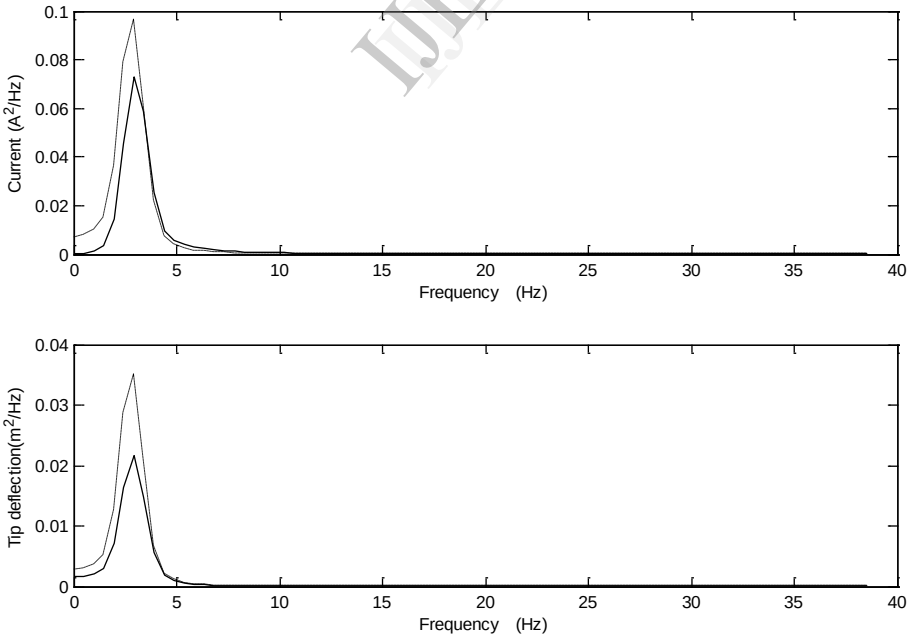

Figure 10. Frequency spectrums of the a) armature current and b) tip deflection Attachment angle $\eta = 0^o$ (-) and $\eta = 45^o$ (-----).

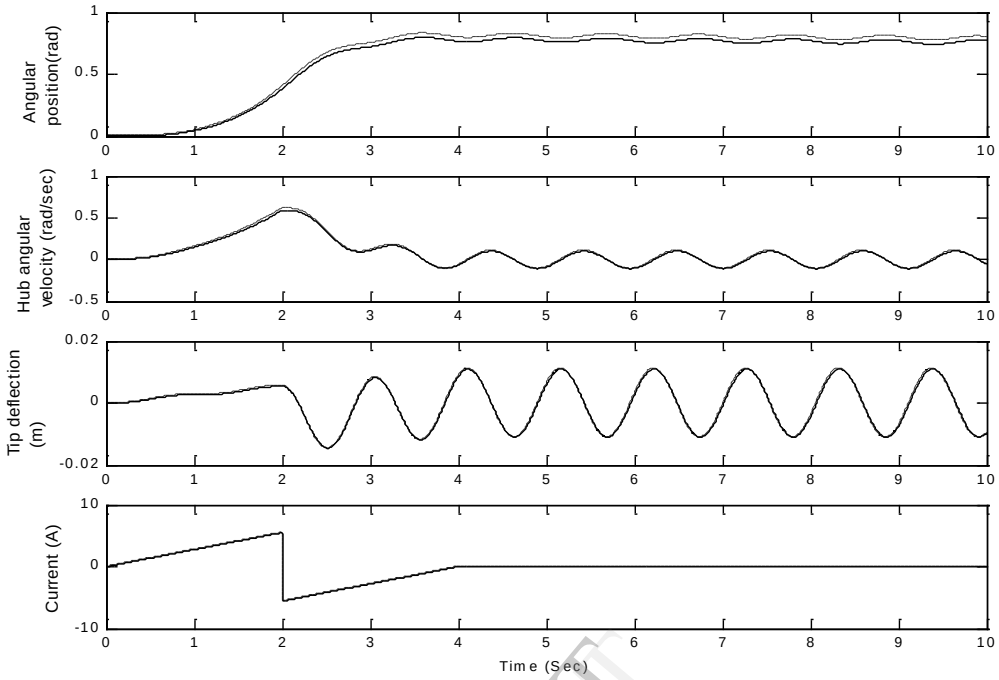

Figure 11. System response for Stiffness ratio K_e = 0.2 and Attachment angle $\eta = 0^o$ (-) and $\eta = 45^O$ (-----).

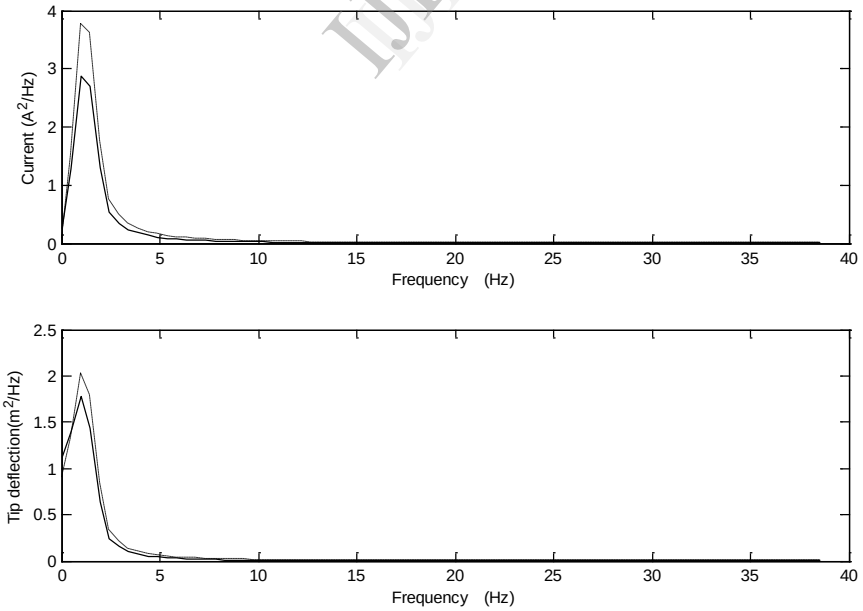

Figure 12. FFT of the current and tip deflection, Attachment angle $\eta = 0^o$ (-) and $\eta = 45^o$ (-----).

6. References

1. L. Shilhansil, "Bending frequencies of a rotating cantilever beam", Journal of Applied Mechanics, 1958, Volume 25, PP.28-30.
2. D. Pruelli, "Natural bending frequency comparable to rotational frequency in rotating cantilever beam", Journal of Applied Mechanics, 1972, Volume 39, PP.602-604..
3. P. W. Likins, "Mathematical modeling of spinning elastic bodies. ",AIAA Journal, 1973, Volume 11(9), xx..
4. K. Kaza and R. Kvaternik, "Non-linear flap-lag-axial equations of a rotating beam", AIAA Journal, 1977, Volume 15 (6), PP.871-874..
5. N. G. Stephens and P. J. Wang, "Stretching and bending of a rotating beam", Journal of Applied Mechanics, 1986, Volume 53, PP.869-872.
6. T. R. Kane, R. R. Ryan and Banerjee A. K, "Dynamics of a cantilever beam attached to a moving base", Journal of Guidance, 1987,Volume 10(2), PP.139-151.
7. H. Baruh and S. K. Tadikonda, "Issues in the dynamics and control of flexible robot manipulators", Journal of Guidance, 1989,Volume 12, PP.659-671..
8. S. K. Tadikonda and H. T. Chang, "On the geometric stiffness in flexible multibody dynamics", Journal of Vibrations and Acoustics, 1995, Volume 117, PP.452-461.
9. A. S. Yigit, A. G. Ulsoy and Scott R. A, "Dynamics of a radially rotating beam with impact, Part 1: Theoretical and computational model", ASME Journal of Vibration and Acoustics, 1990, volume 112, PP.65-70.
10. Y. C. Pan, R. A. Scott and A. G. Ulsoy, "Dynamic modeling and simulation of flexible robots with prismatic joints ", ASME Journal of Mechanical Design, 1990, Volume 112, PP.307-314.
11. K. Kaza and R. Kvaternik, "Non-linear flap-lag-axial equations of a rotating beam", AIAA Journal, 1977, Volume **15** (6), PP.871-874..
12. B. O. Al-Bedoor, "Geometrically non-linear dynamic model of a rotating flexible arm.", Computer Methods in Applied Mechanics and Engineering, 1999, Volume 169, PP. 177-190.
13. B. O. Al-Bedoor and M. N. Hamdan, "Geometrically non-linear dynamic model of a rotating flexible arm", Journal of Sound and Vibration, 2000, Volume **240**, PP. 59-72.
14. Burton, T.D., Introduction to dynamic systems analysis, international edition, McGraw-Hill Book Co., Singapore, 1994.

Appendix A

Constant Coefficients

$$\beta = \frac{EI\lambda^4}{\rho}$$

$$\beta_1 = \frac{1}{3} + \frac{R_H{}^2}{l^2} + \frac{R_H}{l}\cos\eta + a_2\left(1 + \frac{R_H{}^2}{l^2} + 2\frac{R_H}{l}\cos\eta\right) + a_1 + a_3$$

$$\beta_2 = \int_0^1 \phi^2 d\zeta + a_2\phi^2(1) + a_3\phi^{`2}(1)$$

$$\beta_3 = \int_0^1 \phi''^2 d\zeta + 2K_e\phi'^2(\zeta)\Big|_{\zeta=0}.$$

$$\beta_4 = \int_0^1 \phi^2 d\zeta - \int_0^1 \zeta\left(\int_0^\zeta \phi'^2 d\chi\right)d\zeta - \frac{R_H}{l}\cos\eta\int_0^1\left(\int_0^\zeta \phi'^2 d\chi\right)d\zeta + a_2\left(\phi^2(1) - \left(\int_0^\zeta \phi'^2 d\chi\right) - \frac{R_H}{l}\cos\eta\left(\int_0^\zeta \phi'^2 d\chi\right)\right)$$

$$\beta_5 = \frac{1}{4}\left[\int_0^1\left(\int_0^\zeta \phi'^2 d\chi\right)^2 d\zeta - \int_0^1 \zeta\left(\int_0^\zeta \phi'^4 d\chi\right)d\zeta - \frac{R_H}{l}\cos\eta\int_0^1\left(\int_0^\zeta \phi'^4 d\chi\right)d\zeta\right] + \frac{1}{4}a_2\left(\left(\int_0^\zeta \phi'^2 dx\right)^2 - \left(\int_0^\zeta \phi'^4 dx\right)\left(1 + \frac{R_H}{l}\cos\eta\right)\right)\Bigg|_{\zeta=1}$$

$$\beta_6 = 2\left[\int_0^1 \zeta\phi d\zeta + \frac{R_H}{l}\cos\eta\int_0^1 \phi\ \ d\zeta\right] + 2a_2\left[1 + \frac{R_H}{l}\cos\eta\right]\phi\Big|_{\zeta=1} + 2a_3\phi'\Big|_{\zeta=1} \qquad \beta_9 = \int_0^1 \phi'^2\phi''^2 d\zeta$$

$$\beta_7 = \int_0^1 \phi\left(\int_0^\zeta \phi'^2 d\chi\right)d\zeta + a_2\left(\phi\left(\int_0^\zeta \phi'^2 d\chi\right)\right)\Bigg|_{\zeta=1} + a_3\phi'^3\Big|_{\zeta=1} \qquad \beta_8 = \int_0^1\left(\int_0^\zeta \phi'^2 d\chi\right)^2 d\zeta + a_2\left(\int_0^\zeta \phi'^2 d\chi\right)^2\Bigg|_{\zeta=1} + a_3\phi'^4\Big|_{\zeta=1}$$

$$\beta_{10} = -\frac{3}{4}\left[\int_0^1 \phi\left(\int_0^\zeta \phi'^4 d\chi\right)d\zeta + a_2\phi\left(\int_0^\zeta \phi'^4 d\chi\right)\Bigg|_{\zeta=1} - a_3\phi'^5\Big|_{\zeta=1}\right] \qquad \beta_{12} = -\frac{R_H}{l}\sin\eta\left[\int_0^1\left(\int_0^\zeta \phi'^4 d\chi\right)d\zeta + a_2\left(\int_0^\zeta \phi'^4 d\chi\right)\Big|_{\zeta=1}\right]$$

$$\beta_{11} = -2\frac{R_H}{l}\sin\eta\left[\int_0^1\left(\int_0^\zeta \phi'^2 d\chi\right)d\zeta + a_2\left(\int_0^\zeta \phi'^2 d\chi\right)\Big|_{\zeta=1}\right] \qquad \beta_{13} = -2\frac{R_H}{l}\sin\eta\left[\int_0^1 \phi d\zeta + a_2\phi\Big|_{\zeta=1}\right]$$

Where $a_1 = m_H / m_A$, $a_2 = M / m_A$, $a_3 = J_M / [m_A l^2]$ and $K_e = K_t l / [EI]$.